Journal of Cell Science 108, 1063-1069 (1995)
Printed in Great Britain © The Company of Biologists Limited 1995

Scanning force microscopy of microtubules and polymorphic tubulin assemblies in air and in liquid

W. Vater[1], W. Fritzsche[2], A. Schaper[2], K. J. Böhm[1], E. Unger[1] and T. M. Jovin[2,*]

[1]Institut für Molekulare Biotechnologie, Forschungsgruppe Elektronenmikroskopie und Molekulare Zytologie, POB 100813, D-07708 Jena, Germany
[2]Max-Planck-Institut für Biophysikalische Chemie, Abteilung Molekulare Biologie, POB 2841, D-37018 Göttingen, Germany

*Author for correspondence

SUMMARY

We have investigated microtubules (MTs) and polymorphic assemblies, formed in vitro from isolated microtubule protein, by scanning force microscopy (SFM) in air and in liquid. Immobilization of MTs was achieved by placing a drop of the assembly solution on a polylysine-coated coverslip. After washing with taxol and air drying, the characteristic microtubular fibrous morphology appeared in the SFM. The MTs formed a network similar to that obtained by transmission electron microscopy (TEM). A height of ~9.5 nm for dried MTs was computed from the surface topography. Glutaraldehyde fixation of the MTs yielded higher structures (~14 nm), which swelled to ~20 nm after rehydration, a value close to the MT diameter of ~25 nm determined from TEM images of ultrathin sections. The protofilament pattern of the MTs and surface attached MT-associated proteins were not apparent from SFM, although the height along the long axis of the MTs appeared slightly modulated. In addition to MTs, various polymorphic tubulin assemblies including ribbons, hoops and double-walled MTs were visualized by SFM.

Key words: atomic force microscopy, cytoskeleton, microtubule

INTRODUCTION

Microtubules (MTs) are fibrillar structures and ubiquitous components of the cytoskeleton of eukaryotic cells (for an overview see Hyams and Lloyd, 1994). They fulfill essential roles in cell motility, cell division, and intracellular transport processes, and are involved in ciliary and flagellar movement of cells.

The functional versatility of MTs is achieved by dynamic morphological changes of a subfiber, the protofilament, consisting of tubulin heterodimer molecules of alternating α and β globular subunits (4-5 nm in diameter). In the MT the tubulin subunits are aligned 'head-to-tail' in parallel rows along the long axis (for a review see Gelfand and Bershadsky, 1991). Vertebrate MT consists primarily of 13 protofilaments encircling a hollow central core, thereby yielding a tube diameter of ~25 nm. The radial protofilament thickness defining the MT wall thickness is 4.0-5.5 nm from transmission electron microscopy (TEM) (Cohen et al., 1971; Amos and Klug, 1974; Cohen et al., 1975; McEwen and Edelstein, 1980; Amos and Amos, 1991), although for hydrated MTs a wall thickness of 7.5-8.0 nm has been reported from X-ray diffraction and small-angle X-ray scattering (Fedorov et al., 1977; Mandelkow et al., 1977; Amos, 1979). It is possible that the wall shrinks during the preparation procedure for electron microscopy and it is further assumed that the inner and outer edges of the tubule wall are obscured by the stain necessary for electron microscopic contrast, leading to reduced estimations of the wall thickness (McEwen and Edelstein, 1980). In addition, MT-associated proteins (MAPs) binding on the MT surface (Dentler et al., 1975) may also influence the thickness measurements. MAPs are regarded as the major contributors to MT stability in vivo (see e.g. Chapin and Bulinski, 1992).

Depending on the conditions applied, tubulin dimers self-assemble in vitro, leading to polymorphic assemblies including ribbons, hoop-like structures and double-walled MTs (dwMTs) (for a review see Unger et al., 1990). Ribbons consist of metastable flat assemblies of incomplete MT walls and can be induced, e.g. by glycerol (Mandelkow and Mandelkow, 1979), dimethylsulphoxide (Fakhari et al., 1984), or taxol (Schiff et al., 1979). In cross-section they exhibit a C- or S-shaped structure (Burton, 1981; Böhm et al., 1987). A hoop-like morphology appears after association of the lateral edges of ribbons (for structural details see Mandelkow et al., 1984). The generation of dwMTs requires particular polycationic substances, e.g. histones, connecting two layers of tubulin protofilaments (Behnke, 1975; Jacobs et al., 1975; Burton, 1981). From cross-sectional preparations, ~46 nm for the outer diameter and ~15 nm for the wall thickness have been obtained by TEM (Unger et al., 1988).

Scanning probe microscopy (including scanning force, SFM, and scanning tunneling microscopy, STM) is uniquely suited for investigation of the topography of biological specimens at molecular resolution (for reviews see Engel, 1991; Marti and Amrein, 1993). Some attempts have been made to resolve reconstituted MTs by SFM and STM

(Hameroff et al., 1989; Simic-Krstic et al., 1989; Hameroff et al., 1990; Dixon Northern et al., 1992). Despite the existence of numerous well established specimen-preparation techniques for tubulin assemblies, an adaptation for scanning probe microscopy has proven difficult.

In this study we report the SFM imaging of MTs and polymorphic tubulin assemblies in air and in liquid. The latter capability in particular, offers unique opportunities for studying the very dynamic properties of these cytoskeletal elements. The degree of immobilization required for achieving nanometer resolution was provided by the use of polylysine-coated glass.

MATERIALS AND METHODS

Tubulin assemblies

Microtubule protein (tubulin and copurified MAPs) was isolated from fresh porcine brain according to a slightly modified (Vater et al., 1983) procedure of Shelanski et al. (1973). Protein concentrations were determined by the Lowry method (Lowry et al., 1951). MTs were obtained from assembly solution (1 mg/ml of microtubule protein in 20 mM 2(*N*-morpholino) ethanesulfonic acid (MES), 80 mM NaCl, 1 mM ethylenebis(oxyethylenenitrilo) tetraacetate, 0.5 mM $MgCl_2$, 0.36 mM GTP, pH 6.4) after incubation at 37°C for 30 minutes. MTs formed under these conditions have predominantly 14 protofilaments (Böhm et al., 1984). Ribbons and hoop-like tubulin assemblies were induced by adding taxol (10 μM) to the assembly solution; dwMTs were obtained after reconstitution in the presence of 0.1, 0.25, and 0.5 mg/ml histone H1 (Boehringer, Ingelheim, FRG). The assembly products were examined in the SFM immediately after formation.

Sample preparation for scanning force microscopy

A glass coverslip (Plano, Marburg, FRG) cleaned by ultrasonication was pretreated by placing a 50 μl drop of polylysine (1 mg/ml, poly-L-lysine·Br, 6-9 kDa, Serva, Heidelberg, FRG, in double distilled water) on the surface for 2 minutes. The excess polylysine solution was removed with a filter paper and replaced by a 50 μl drop of the assembly product, which was likewise blotted off after 2 minutes of incubation. The surface was washed twice with 50 μl drops of 20 μM taxol in double distilled water. Excess liquid was soaked up with a filter paper and the specimen was air dried. For MT fixation the assembly product was treated with 1% glutaraldehyde for 10 minutes prior to placing the drop on the coverslip.

Scanning force microscopy

SFM measurements were performed with a contact NanoScope III (Digital Instruments (DI), Santa Barbara, CA) under ambient conditions (19-25°C temperature, 15-50% relative humidity). The microscope was equipped with a J-scanner with 135 μm×135 μm×5.5 μm (x,y,z) scan range. Triangular cantilevers with integrated Si tips and force constants of ~0.06 N/m were used (Ultralevers, Park Scientific Instruments, Sunnyvale, CA). Scanning was performed at ~8 Hz in the topographic (isoforce) mode at a minimum loading force typically in the nN range. SFM imaging in liquid was with a fluid cell (DI) and the fixed samples were rehydrated in phosphate-buffered saline (PBS). The SFM images (512×512 pixels) were processed with the NanoScope software and with the programs Photoshop (Adobe Systems) and Canvas (Deneba Systems) for presentation. The reported lateral dimension of a surface feature is the full width at half-maximum height determined by the sectioning software of the NanoScope.

Transmission electron microscopy

For TEM the assembly product was either adsorbed on a polylysine-coated carbon/Formvar grid and negatively stained with 1% uranyl acetate in double distilled water or resin embedded and ultrathin sectioned as described elsewhere (Jelke et al., 1987). The specimen was examined in a Philips STEM 400 T (Philips, Eindhoven, NL) transmission electron microscope.

RESULTS

Microtubules

We investigated the topography of MTs after adsorption on polylysine-coated glass. Polylysine was essential for the retention and stability of MTs and stable imaging by SFM was routinely achieved on such surfaces. Fig. 1A shows a typical field of unfixed air dried MTs. The latter appeared in a slightly curved fibrous morphology with randomized orientations and with several cross contacts (fibrillar network). Fig. 1B presents a perspective view of a surface area from which the microtubular dimensions could be obtained (Fig. 1C,D,E), i.e. a height of 9-10 nm and a width of 70-100 nm. These values deviate significantly from the MT dimensions derived from TEM (see Discussion below). The points of MT crossing-over were elevated by ~9 nm, corresponding to the height of a dried MT. The stacking orientation of the crossed MTs, however, could not be resolved from the dried specimen. In Fig. 1A,B round protrusions 60-80 nm in width and 20-30 nm in height also appeared on the polylysine surface, presumably formed by nonassembled and/or denatured tubulin aggregates (see e.g. Keates, 1980). Fig. 1F shows a single MT at higher magnification. The MT surface appeared slightly modulated along its longitudinal axis with surface corrugations of 1-2 nm in height occurring with periodicities of 40-50 nm along the microtubule length.

MTs adsorbed on a polylysine-coated grid were investigated in parallel by TEM. In the whole mount preparation (Fig. 2A) a pattern was evident, similar to that in Fig. 1A. At higher magnification, however, a longitudinal striation appeared in the MT (Fig. 2B), reflecting a protofilament substructure (see e.g. Langford, 1980) that was not resolvable by SFM. Longitudinally sectioned MTs (~25 nm in diameter) with MAPs protruding from the MT surface are shown in Fig. 2C. Both the protofilament arrangement and the attached MAPs may be responsible for the MT surface corrugations seen by SFM (Fig. 1F).

Polymorphic assemblies: hoops, ribbons and double-walled microtubules

A collection of different tubulin assemblies air dried and imaged by SFM is shown in Fig. 3. Ribbons, hoops (Fig. 3A) and the more complex dwMTs are represented (Fig. 3B,C). The hoops (Fig. 3A,*h*) coexisted with ribbons (Fig. 3A,*r*); both were ~4.5 nm in height, i.e. half the height of the air dried MT. Fig. 3B shows a mixed population of MTs and dwMTs formed in the presence of 0.1 mg/ml histone H1. The dwMTs had a width similar to that of dried MTs and a height of 16.5-20.0 nm, corresponding to about twice the height of dried MTs. In addition, some broader structures, presumably comprising two or more dwMTs, could be resolved. At 0.25 mg/ml H1 large bundles of dwMTs were formed (Fig. 3C), whereas at 0.5 mg/ml (data not shown) only short dwMTs appeared together with many granular background contaminations that were formed most probably from amorphous H1/tubulin aggregates (Unger et al., 1988).

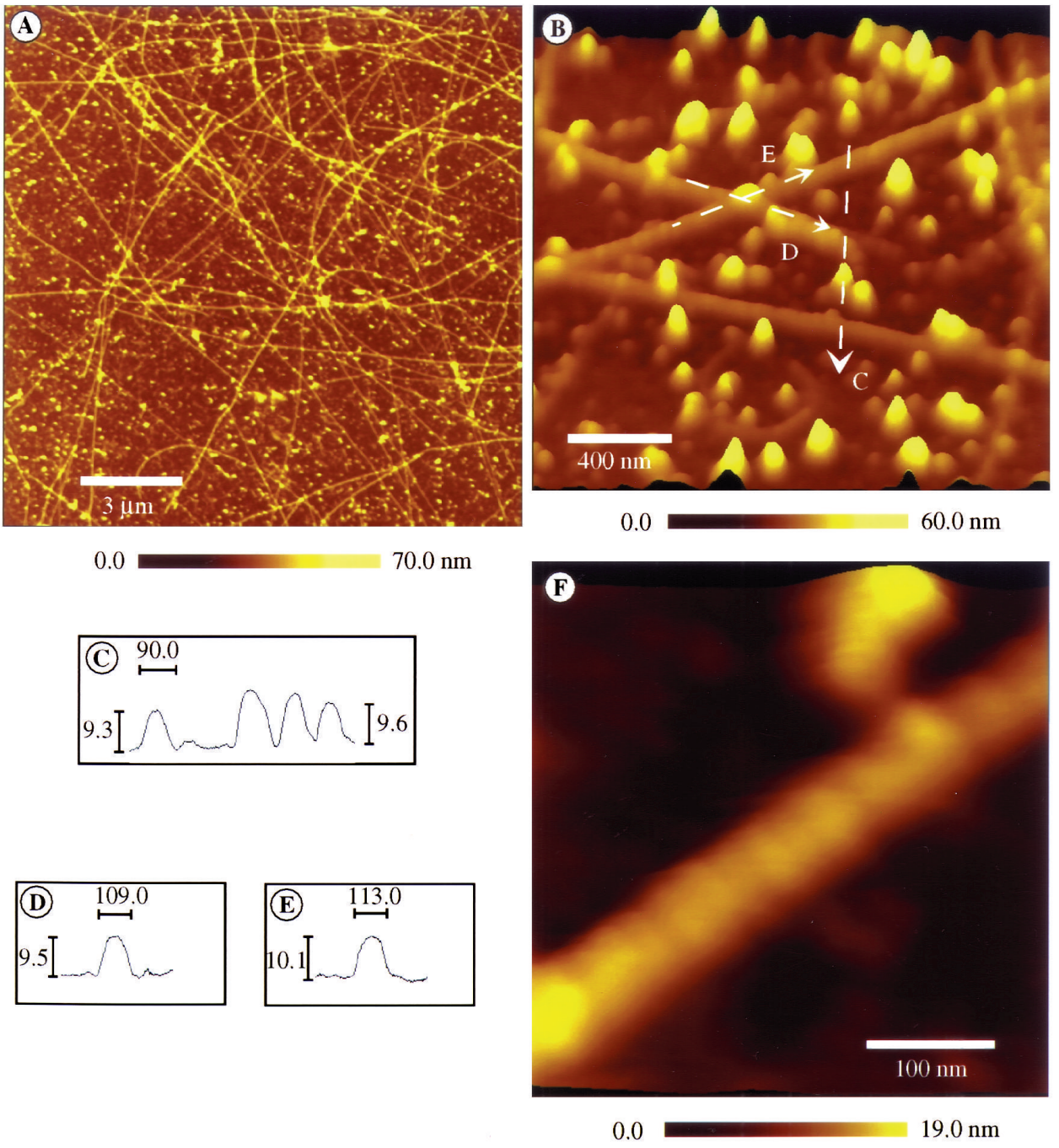

Fig. 1. MTs in the SFM. The height is color coded according to the horizontal bars. (A) A typical field of MTs adsorbed on polylysine-coated glass and air dried. (B) Surface plot of a zoomed area. Tilt angle 75°. (C,D,E) Surface profiles along the lines drawn in B. Height and width are in nm. (F) Zoom and surface plot of a single MT. Tilt angle 80°. The MT surface appears slightly modulated along the longitudinal axis.

Imaging microtubules in liquid

SFM imaging in liquid was successful with fixed and rehydrated MTs. Fig. 4A,B shows a selected area of fixed MTs imaged in air and in PBS buffer. Since the tips were irreversibly contaminated immediately after their engagement on the dried specimen, most probably due to an uptake of loosely bound material, the images were blurred and the structures appeared broader (the MT diameter exceeded 140 nm). For fixed and air dried MTs, a height of ~14 nm was measured in selected sample regions (an example is shown in Fig. 4A, lower right corner), a value significantly higher than for the unfixed MTs. After rehydration, swelling of the fixed MTs occurred up to ~20 nm in height (Fig. 4B, inset, lower right corner). In other surface regions the height of fixed MTs was difficult to measure due to the reduced topographic contrast. Zooms of regions of overlapping MTs are presented in Fig. 4A,B (insets, upper left corners). Fig. 4B clearly shows two parallel MTs on top of a single MT. In contrast, the stacking

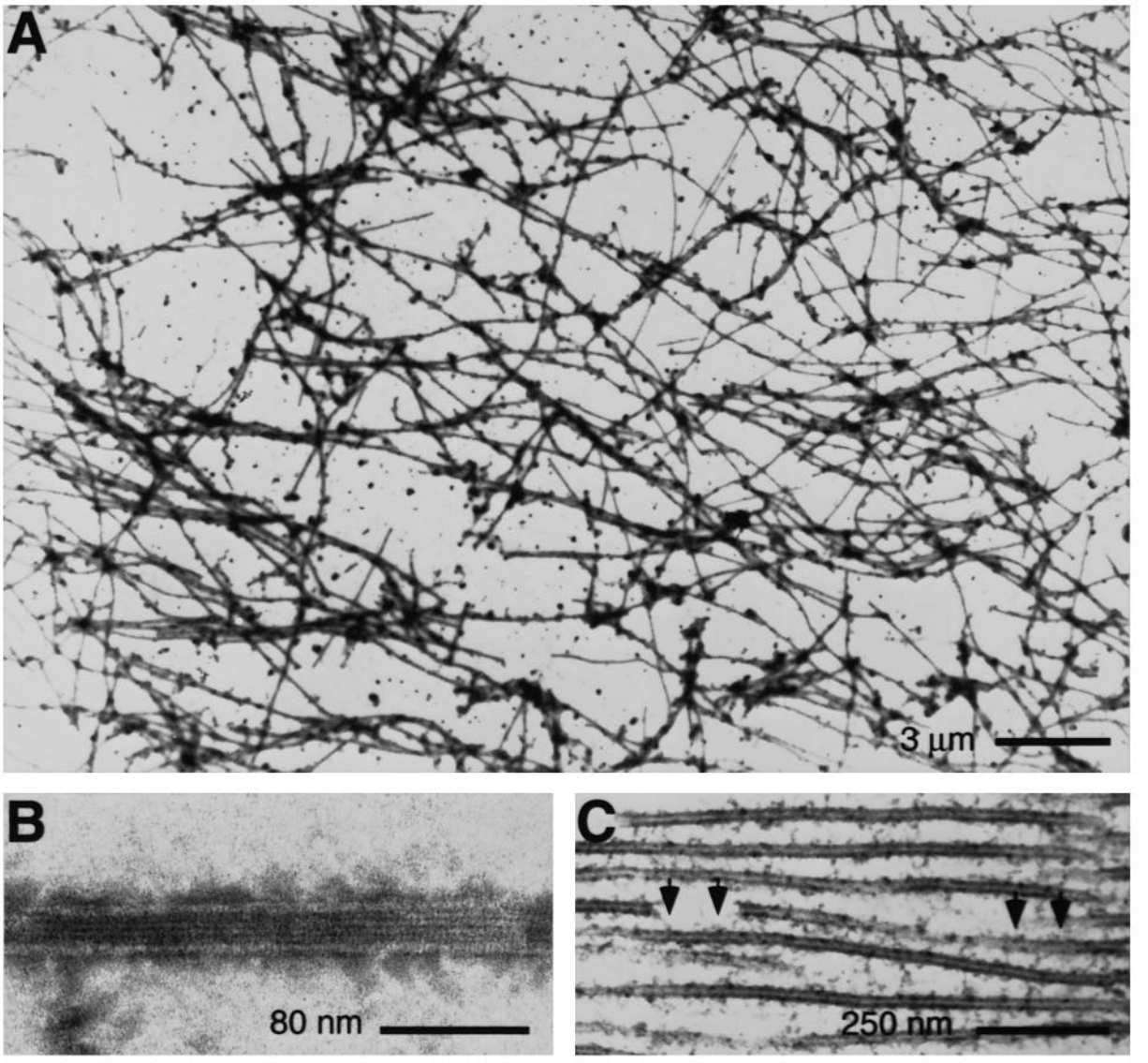

Fig. 2. MTs in the transmission electron microscope. (A) MTs immobilized on polylysine-coated carbon/Formvar grids and after contrast enhancement. Overview. (B) MTs at higher magnification. The longitudinal striation pattern is due to the protofilament substructure. (C) Ultrathin section of resin-embedded fixed MTs that were sliced along their longitudinal axis.The MAPs extend from the MT surface. Examples are indicated by arrowheads.

orientation was not resolvable in the dried state (Fig. 4A). The height of the crossing point was ~30 nm, somewhat lower than expected for the stacking of two rehydrated MTs. This may have arisen in this case due to an elastic depression induced by the tracking SFM tip.

DISCUSSION

Structural implications of the tubulin assembly dimensions derived from scanning force microscopy

In this study we successfully imaged MTs by SFM in air and in liquid. Different assembly products were clearly distinguished and structural details were revealed with a resolution of several nanometers. The structural implications of our MT data are summarized in Fig. 5. For the unfixed and dried MTs the height was ~9.5 nm (Fig. 1C). This value is less than twice the wall thickness of a native MT (Fedorov et al., 1977; Mandelkow et al., 1977; Amos, 1979). We conclude that the MT collapses and the wall shrinks (Fig. 5A), as in the negative staining procedure for TEM (McEwen and Edelstein, 1980). The flattening occurring as a consequence of the collapse could in part explain the large apparent width of the MT. After glutaraldehyde fixation and air drying the MT height was greater (~14 nm, Fig. 4A), which could be due to prevention of shrinkage by protein crosslinking leading to a retention of the native wall thickness despite collapse of the tube (Fig. 5B). After rehydration of the fixed MTs the height increased up to ~20 nm (Fig. 4B), indicating a partial restoration of the hollow tube structure (Fig. 5C). Neither the protofilament structure of the MT nor the associated MAPs observed after negative

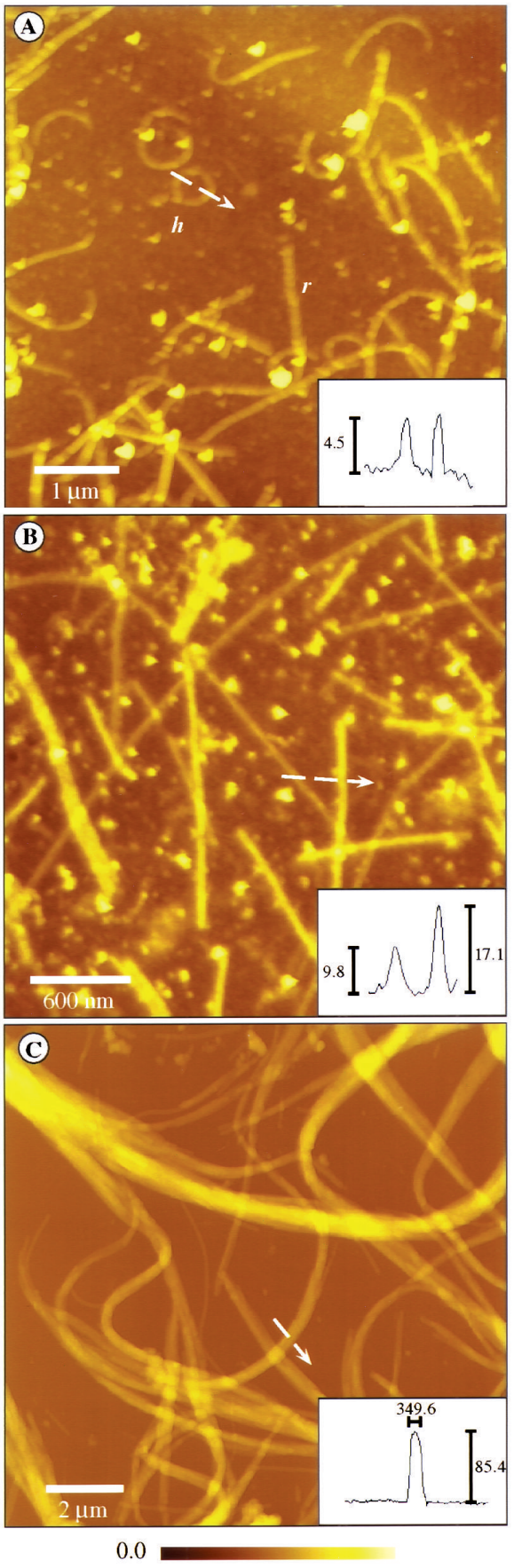

Fig. 3. SFM of polymorphic tubulin assemblies. (A) Ribbons (*r*) and hoop-like structures (*h*) formed in the presence of taxol. Color bar, 30 nm. Inset: surface profile through a hoop along the broken line. (B) MTs and dwMTs coexist after assembly in the presence of histone H1 (0.1 mg/ml). Color bar, 50 nm. Inset: surface profile along the broken line crossing a MT and a dwMT. (C) Bundles of dwMTs appeared with 0.25 mg/ml H1. Color bar, 520 nm. Inset: surface profile along the broken line.

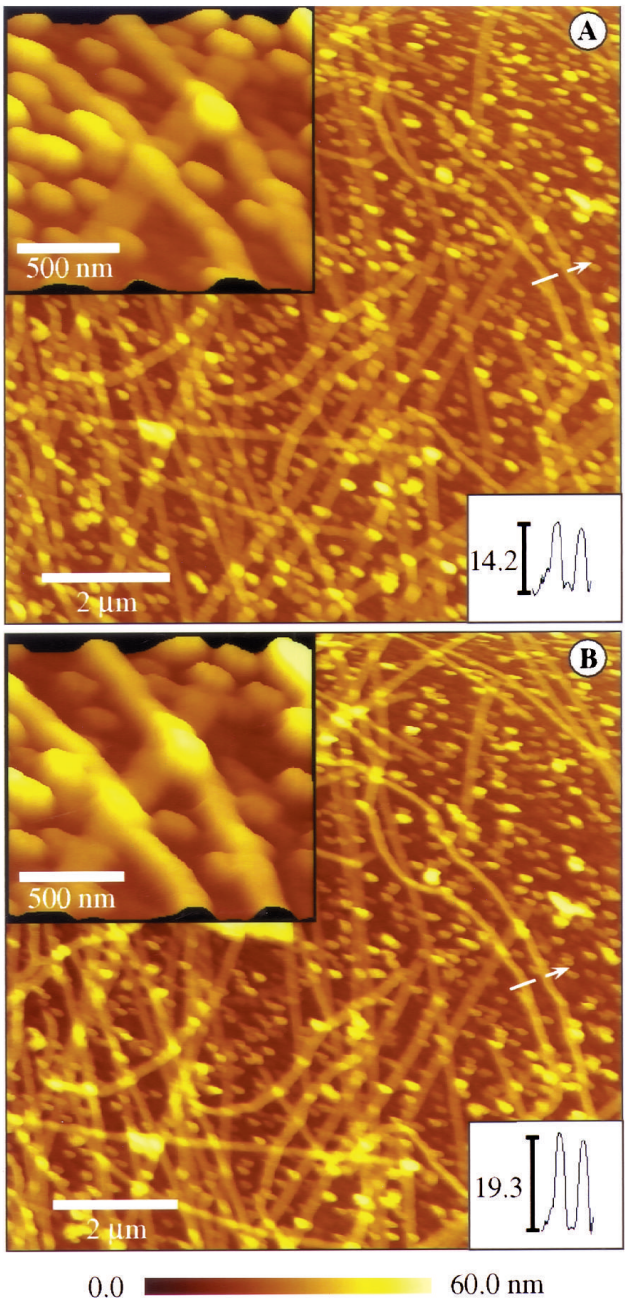

Fig. 4. SFM micrograph of glutaraldehyde-fixed MTs in air and in liquid. Top views. (A) Topography of the air-dried sample. Upper left inset, perspective view of the area at the arrow in A; lower right inset, cross-section along the arrow in A. (B) The same surface area as shown in A but after rehydration. Same notation as in A.

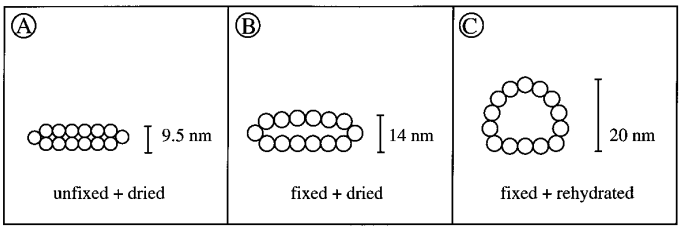

Fig. 5. Structural implications of the MT heights from SFM metrology under different experimental conditions. A single circle represents a cross-section of a tubulin protofilament. MT cross-section under the conditions: (A) unfixed and air dried; (B) fixed and air dried. The fixed proteins do not shrink as in (A) and are therefore represented by larger circles; (C) fixed and rehydrated structure. See text for further discussion.

staining (Fig. 2B) and section preparation (Fig. 2C) for the TEM were resolvable by SFM. However, the MT surface exhibited some corrugations (Fig. 1F), possibly due to the attached MAPs and/or reflecting the intrinsic protofilament substructure.

SFM was also applied to the investigation of several polymorphic assemblies. Hoops (height ~4.5 nm) were easily detectable by their characteristic shape, whereas ribbons could be differentiated from MTs only by their height of ~4.5 nm, about half that of MTs. For dwMTs heights of 16.5-20 nm were determined, indicating values distinctly less than twice the wall thickness of dwMTs (Unger et al., 1988). We assume that not only the inner MT but also the H1 intermediate layer collapses and shrinks during air drying. The protofilament architecture was also not evident in the polymorphic structures. In comparing the contrast in SFM and TEM one has to take into account that in TEM the electron beam traverses the entire object, i.e. yielding a two-dimensional projection of the object's electron density map including also inner surfaces. In contrast, SFM images reveal the equiforce surface topography of the outer boundary (interface) of the object. Thus, the techniques are distinct but complementary.

Present limits of structural resolution in scanning force microscopy of tubulin assemblies

Successful imaging of the MT substructure requires a subnanometer resolution capability in the SFM. Despite the fundamental dysfunctions in the mechanisms of contrast generation emphasized above, the lower lateral resolution of SFM compared to electron microscopy is mainly due to the finite tip profile, which limits the resolution to ~10 nm. We used etched Si tips produced by state-of-the-art microfabrication technology, which in our experience exhibit the highest structural resolution reproducibly achievable in single particle detection (Schaper et al., 1993, 1994). Structural broadening due to tip-sample convolution is a well known effect in SFM (see e.g. Keller, 1991; Bustamante et al., 1992; Fritzsche et al., 1994; Pietrasanta et al., 1994); that is, the tip profile limits the higher spatial frequencies. Another problem related to the resolution power of the SFM is the sensitivity of the cantilever, since the contact forces between the tip and a surface area can induce elastic depression (or even plastic deformation) of soft materials, such as biological specimens, thereby yielding a systematic underestimation of the height (or even destruction of the surface relief). Elasticity is difficult to measure in the standard continuous contact mode of the microscope. The situation is more complicated when imaging in air, which introduces substantial capillary forces due to the surface humidity. The magnitude of the contact force also depends critically on the compliance of the cantilever (bending force) and on the physical chemical properties of the tip material. Last, but not least, shearing forces induced by tip tracking can be involved. For that reason we have also performed SFM imaging of MTs in the tapping mode (DI, for details see e.g. Delain et al., 1992) in which the tip is in discontinuous (cyclic) contact with the surface area ('woodpecker mode'). Similar MT dimensions were obtained (data not shown), from which we conclude that shearing forces do not contribute significantly to the systematic underestimation of the MT height (Fig. 4B). Recently, viscoelastic measurements on soft materials were reported that may offer a better understanding of the elastic properties of biomaterials on the nanometer scale (Radmacher et al., 1993). We believe that further improvements in tip and cantilever fabrication should increase the resolution power of SFM by at least one order of magnitude.

SFM in its present state can be applied to the rapid inspection of tubulin assemblies formed under various reassembly conditions. The main advantage of SFM is the potential for imaging MTs in liquid, i.e. under near native conditions. The experiments in an aqueous environment presented in this study are the first step towards this goal. The rehydrated MTs withstand the loading force of the tip, at least to some extent, such that swelling behavior is apparent. This is due to the rehydration of the structure and/or to the drastic reduction of capillary forces in the tip-sample contact. Further progress in the SFM imaging of MTs and other tubulin assemblies will require a method for mounting the samples on a solid support, thereby retaining their native properties. Other topics of interest for SFM studies of tubulin polymorphism are the structure-function relations of the assembly process, e.g. association/dissociation of tubulin forming MTs, and the processes that take place on the MT surface, e.g. the movement of motor proteins along the tubulin lattice (Warner and McIntosh, 1989; Scholey, 1993; Mercer et al., 1994).

We thank M. Kittler for technical assistance. This work was supported by the German Research Council (DFG) (Jo/105-9).

REFERENCES

Amos, L. A. and Klug, A. (1974). Arrangement of subunits in flagellar microtubules. *J. Cell Sci.* **14**, 523-549.

Amos, L. A. (1979). Structure of microtubules. In *Microtubules* (ed. K. Roberts and J. S. Hyams), pp. 1-64. London: Academic Press.

Amos, L. A. and Amos, W. B. (1991). Properties of tubulin. In *Molecules of the Cytoskeleton* (ed. J. Skidmore), pp. 117-141. Houndsmills, Basingstoke, Hampshire, London: Macmillan Education Ltd.

Behnke, O. (1975). An outer component of microtubules. *Nature* **257,** 709-710.

Böhm, K. J., Vater, W., Fenske, H. and Unger, E. (1984). Effect of microtubule-associated proteins on the protofilament number of microtubules assembled in vitro. *Biochim. Biophys. Acta* **800**, 119-126.

Böhm, K. J., Vater, W., Steinmetzer, P. and Unger, E. (1987). Structural dynamics within populations of microtubules and protofilament ribbons. *Biochim. Biophys. Acta* **929**, 154-163.

Burton, P. B. (1981). Polymorphic assemblies of tubulin. In *Cell and Muscle Motility*, vol. 1 (ed. R. M. Dowben and J. M. Shay), pp. 289-333. New York: Plenum Publishing Company.

Bustamante, C., Vesenka, J., Tang, C. L., Rees, W., Guthold, M. and Keller, R. (1992). Circular DNA molecules imaged in air by scanning force microscopy. *Biochemistry* **31**, 22-26.

Chapin, S. J. and Bulinski, J. C. (1992). Microtubule stabilization by assembly-promoting microtubule-associated proteins: a repeat performance. *Cell Motil. Cytoskel.* **23**, 236-243.

Cohen, C., Harrison, S. C. and Stephans, R. E. (1971). X-ray diffractions from microtubules. *J. Mol. Biol.* **59**, 375-380.

Cohen, C., DeRosier, D., Harrison, S. C., Stephens, R. E. and Thomas, J. (1975). X-ray patterns from microtubules. *Ann. NY Acad. Sci.* **253**, 53-59.

Delain, E., Fourcade, A., Poulin, J. C., Barbin, A., Coulaud, D., Lecam, E. and Paris, E. (1992). Comparative observations of biological specimens, especially DNA and filamentous actin molecules in atomic-force, tunneling and electron-microscopes. *Microsc. Microanal. Microstruct.* **3**, 457-470.

Dentler, W. L., Granett, S. and Rosenbaum, J. L. (1975). Ultrastructural localization of the high molecular weight proteins with in vitro-assembled brain microtubules. *J. Cell Biol.* **65**, 237-241.

Dixon Northern, B. L., Jordan, M. A., Wilson, L. and Zasadinski, J. A. N. (1992). Imaging cellular microtubules with the atomic force microscope. *Proceedings of the Society of Photo-Optical Instrumentation Engineers* **1639**, 138-144.

Engel, A. (1991). Biological applications of scanning probe microscopes. *Annu. Rev. Biophys. Biophys. Chem.* **20**, 79-108.

Fakhari, S. M., Taylor, D. L., Burton, P. R. and Himes, R. H. (1984). The influence of microtubule associated proteins on the production of polymorphic products from tubulin and microtubules. *Cell Biol. Int. Rep.* **8**, 1041-1050.

Fedorov, B. A., Shpungin, I. L., Gelfand, V. I., Rosenblat, V. A., Damaschun, G., Damaschun, H. and Papst, M. (1977). A study of microtubule structures in solution by small-angle X-ray scattering. *FEBS Lett.* **84**, 153-155.

Fritzsche, W., Schaper, A. and Jovin, T. M. (1995). Scanning force microscopy of chromatin fibers in air and in liquid. *Scanning* (in press).

Gelfand, V. I. and Bershadsky, A. D. (1991). Microtubule dynamics: mechanism, regulation, and function. *Annu. Rev. Cell Biol.* **7**, 93-116.

Hameroff, S. R., Simic-Krstic, J., Kelley, M. F., Voelker, M. A., He, J. D., Dereniak, E. L., McCuskey, R. S. and Schneiker, C. W. (1989). Scanning tunneling microscopy of biopolymers - conditions for microtubule stabilization. *J. Vac. Sci. Technol. A* **7**, 2890-2894.

Hameroff, S., Simic-Krstic, Y., Vernetti, L., Lee, Y. C., Sarid, D., Wiedmann, J., Elings, V., Kjoller, K. and McCuskey, R. (1990). Scanning tunneling microscopy of cytoskeletal proteins - microtubules and intermediate filaments. *Journal of Vacuum and Science Technology A* **8**, 687-691.

Hyams, J. S. and Lloyd, C. W. (1994). *Microtubules*. New York: John Wiley.

Jacobs, M., Bennett, P. M. and Dickens, M. J. (1975). Duplex microtubule is a new form of tubulin assembly induced by polycations. *Nature* **257**, 707-709.

Jelke, E., Oertel, B., Böhm, K. J. and Unger, E. (1987). Tubular cytoskeletal elements in sporangia and zoospores of *Phytophthora infestans* (Mont.) DeBary (Oomycetes, Pythiacea). *J. Basic Microbiol.* **27**, 223-228.

Keates, R. A. B. (1980). Effect of glycerol on microtubule polymerization kinetics. *Biochem. Biophys. Res. Commun.* **97**, 1163-1169.

Keller, D. (1991). Reconstruction of STM and AFM images distorted by finite-size tips. *Surf. Sci.* **253**, 353-364.

Langford, G. M. (1980). Arrangement of subunits in microtubules with 14 protofilaments. *J. Cell Biol.* **87**, 521-526.

Lowry, O. H., Rosebrough, N. J., Farr, A. L. and Randall, R. J. (1951). Protein measurement with the phenol reagent. *J. Biol. Chem.* **193**, 265-275.

Mandelkow, E., Thomas, J. and Cohen, C. (1977). Microtubular structure at low resolution by x-ray diffraction. *Proc. Nat. Acad. Sci. USA* **74**, 3370-3374.

Mandelkow, E., Schultheiss, R. and Mandelkow, E.-M. (1984). Assembly and three-dimensional image reconstruction of tubulin hoops. *J. Mol. Biol.* **177**, 507-529.

Mandelkow, E.-M. and Mandelkow, E. (1979). Junctions between microtubule walls. *J. Mol. Biol.* **129**, 135-148.

Marti, O. and Amrein, M. (1993). *STM and SFM in Biology*. New York: Academic Press.

McEwen, B. and Edelstein, S. T. (1980). Evidence for a mixed lattice in microtubules assembled in vitro. *J. Mol. Biol.* **138**, 123-145.

Mercer, J. A., Albanesi, J. P. and Brady, S. T. (1994). Molecular motors and cell motility in brain. *Brain Pathol.* **4**, 167-179.

Pietrasanta, L. I., Schaper, A. and Jovin, T. M. (1994). Imaging subcellular structures of rat mammary carcinoma. *J. Cell Sci.* **107**, 2427-2437.

Radmacher, M., Tillmann, R. W. and Gaub, H. E. (1993). Imaging viscoelasticity by force modulation with the atomic force microscope. *Biophys. J.* **64**, 735-742.

Schaper, A., Pietrasanta, L. I. and Jovin, T. M. (1993). Scanning force microscopy of circular and linear plasmid DNA spread on mica with a quaternary ammonium salt. *Nucl. Acids Res.* **21**, 6004-6009.

Schaper, A., Starink, J. P. P. and Jovin, T. M. (1994). Scanning force microscopy of DNA in air and in liquid using new spreading agents. *FEBS Lett.* **355**, 91-95.

Schiff, P. B., Fant, K. and Horwitz, S. B. (1979). Promotion of microtubule protein assembly in vitro by taxol. *Nature* **277**, 665-667.

Scholey, J. M. (1993). *Motility Assays for Motor Proteins*. New York: Academic Press.

Shelanski, M. L., Gaskin, F. and Cantor, C. R. (1973). Microtubule assembly in the absence of added nucleotides. *Proc. Nat. Acad. Sci. USA* **70**, 765-768.

Simic-Krstic, Y., Kelley, M., Schneiker, C., Krasovich, M., McCuskey, R., Koruga, D. and Hameroff, S. (1989). Direct observation of microtubules with the scanning tunneling microscope. *FASEB J.* **3**, 2184-2188.

Unger, E., Böhm, K. J., Müller, H., Grossmann, H., Fenske, H. and Vater, W. (1988). Formation of double walled microtubules and multilayered tubulin sheets by basic proteins. *Eur. J. Cell Biol.* **46**, 98-104.

Unger, E., Böhm, K. J. and Vater, W. (1990). Structural diversity and dynamics of microtubules and polymorphic tubulin assemblies. *Electron Microsc. Rev.* **3**, 355-395.

Vater, W., Böhm, K. J. and Unger, E. (1983). Effects of DNA on the taxol stimulated in vitro assembly of microtubule protein from porcine brain. *Studio Biophys.* **97**, 49-60.

Warner, F. D. and McIntosh, J. R. (1989). *Kinesin, Dynein and Microtubule Dynamics*. New York: Alan R. Liss.

(Received 26 September 1994 - Accepted 29 November 1994)